

Descriptor: Context-Aware Collaborative Perception in Autonomous Driving Dataset (ConVeX)

*Original*

Descriptor: Context-Aware Collaborative Perception in Autonomous Driving Dataset (ConVeX) / Palena, Marco; Selvaraj, Dinesh Cyril; Chiasserini, Carla Fabiana; Cerquitelli, Tania. - In: IEEE DATA DESCRIPTIONS. - ISSN 2995-4274. - (2026).

*Availability:*

This version is available at: 11583/3010047 since: 2026-04-17T15:51:54Z

*Publisher:*

IEEE

*Published*

DOI:

*Terms of use:*

This article is made available under terms and conditions as specified in the corresponding bibliographic description in the repository

*Publisher copyright*

IEEE postprint/Author's Accepted Manuscript

©2026 IEEE. Personal use of this material is permitted. Permission from IEEE must be obtained for all other uses, in any current or future media, including reprinting/republishing this material for advertising or promotional purposes, creating new collecting works, for resale or lists, or reuse of any copyrighted component of this work in other works.

(Article begins on next page)

# The PVZEN Lab for Energy Communities: Monitoring System for Identification of Photovoltaic/Battery/Converter Energy Models

Angela Amato, Alessio Carullo, Alessandro Ciocia, Simone Corbellini, Filippo Spertino,  
Alberto Vallan,  
Marco Augusto Alfredo Bertolasco

*Abstract*—The main topic of this article is the PhotoVoltaic Zero Energy Network (PVZEN) laboratory, which is an energy community for research purposes established at the Politecnico di Torino campus. The PVZEN laboratory has three users, each equipped with a PhotoVoltaic (PV) generator, lithium batteries with proper electronic converters, and emulators of electric appliances, including heat pumps. These users are capable of exchanging energy based on specific strategies conceived for maximizing the use of renewable energy sources. This work is focused on the identification of energy models that can describe the main components of the community. With the aim of providing reliable models that can enable other researchers in simulating the microgrid in different operating conditions, a monitoring system has been installed close to the relevant commercial devices, to obtain traceable measurements of electrical and environmental quantities. The reference results provided by the monitoring system allowed the multi-meter internal to the inverters to be characterized. Furthermore, the DC measurements provided by the monitoring system allowed reliable models to be identified for PV generators and storage systems. For the former, the identified models exhibited root means square errors between measured and predicted energy lower than 1 % during a time interval of about three months; for the latter, charge and discharge efficiencies and self-discharge were in agreement with expected values for the lithium batteries.

## I. INTRODUCTION

THE new paradigm of energy communities in the energy sector enables local authorities, companies and private citizens to share energy production from renewable sources according to directives 2018/2001/EU and 2019/944/EU, within the “Clean Energy for All Europeans Package” [1], [2]. These directives are intended to promote the self-consumption of energy from renewable sources for developing a local energy trade. The number of pilot projects in this scenario has increased since European Union (EU) members started receiving these directives and the analysis of energy communities in 29 EU countries in 2022 can be found in [3]. Almost ten thousand energy communities are present in Europe and almost half of them are in Germany. An example is the village of Feldheim, where a localized energy system based on wind turbines, PhotoVoltaic (PV) generators, and biogas is in operation [4]. Another example is Samsø, a Danish island, which has reached carbon neutrality by significantly reducing its CO<sub>2</sub> emissions thanks to different sustainable technologies, such as on-shore and off-shore wind turbines, biomass-fueled district heating, solar systems, electric vehicles [5]. Ecoisola, which is located in Salina Island in Italy, is a pioneering energy community that effectively meets its energy requirements through the integration of PV and wind power plants, energy storage systems, and demand response strategy [6]. In general, most of the energy communities employ PV systems and electrochemical batteries, thus highlighting the importance of these two technologies.

In the framework of energy communities, this paper deals with the PhotoVoltaic Zero Energy Network (PVZEN) laboratory, which is a micro-grid established at the Politecnico di Torino campus. The present paper focuses on the purpose of “energy community digital twin”, which can be used by researchers in any site for PV generators, with reasonable number of users and with any load power profile. Such a digital twin needs a metrological characterization of the PVZEN components, thus requiring an *ad-hoc* monitoring system that can provide traceable measurements of electrical quantities in Direct Current (DC) and Alternating Current (AC). In particular, the measurements provided by the multi-meters embedded inside the commercial power converters are compared to the measurements performed by a specifically designed data-acquisition system, which acts as a reference both for electrical and environmental quantities.

This paper is the extended version of the I<sup>2</sup>MTC-2024 conference paper [7] and is organized as follows. Section II shows a review on the energy modelling of microgrid components. In section III, the description of the architecture of the PVZEN laboratory and the details about the models that simulate the main components are provided. Section IV describes the reference data-acquisition system and its metrological performance, while section V describes the methodology used to identify the parameters of the models involved. Section VI reports experimental results, which refer both to

the metrological characterization of the components of the PVZEN laboratory and the model identification process. The conclusions are summarized in Section VII.

## II. REVIEW ON ENERGY MODELLING OF MICROGRID COMPONENTS

The novelty of the present paper is the combined effort in optimizing energy models for different microgrid components, e.g., photovoltaic systems, lithium batteries, and converters, and in providing traceable measurements supporting these energy models. In fact, this paper provides information about the measurement systems, calibration details and uncertainty evaluation, useful for the replicability of the proposed procedure. Moreover, measurements from the PV converters are compared to measurements obtained with the system calibrated by the authors. In this Section, a review related to the modelling of the above-mentioned microgrid components is presented, with a special focus on the qualification of measurements in terms of uncertainty.

Regarding the modelling of PV generators, the literature review shows that papers generally do not provide adequate information about measurement uncertainty and traceability. The models can be subdivided into two main groups. The first group includes papers based on models that directly estimate the DC power at the Maximum Power Point (MPP) without calculating the entire current-voltage ( $I$ - $V$ ) curve [8,9]. These “DC models” use simplified equations where power is proportional to irradiance [10], incorporating corrections for the losses due to temperature [11] and low irradiance [12]. The second group includes papers that rely on diode-based models [13], simulating the operation of PV arrays as equivalent circuits, such as single-diode or multi-diode configurations [14][15]. Although they offer higher estimation accuracy, they require high computational effort and are less used in microgrid simulations with respect to “DC models”. Moreover, a comparison between them in [16] showed that, for energy modeling, the use of a “DC model” is the best compromise between accuracy and computation effort.

A common approach for the improvement of the DC model is the comparison of the simulated generation profiles and the measured data [17]. In [18], each parameter of the double diode model is calculated with formulae that use different parts of the measured  $I$ - $V$  curve: for example, the points close to short circuit condition are used for the calculation of the shunt resistance. In [19], a similar approach is used that relies on a regression model. A different method is proposed in [8]: in this case, the DC theoretical model is modified by changing the value of the model parameters, or adding new formulae, to minimize the differences between measurements and simulations (e.g., the root mean square value). Nevertheless, in [8] the optimization of the model is done including also the DC/AC conversion efficiency and all the other sources of losses in the systems (e.g., the transformer), because few details are available about the analyzed plants.

On the other hand, the research papers focusing on the data acquisition of microgrid components are generally lacking in the models and their optimization. For example, article [20] proposes a real-time monitoring system for PV panels and incorporates uncertainty quantification in the measurement process. Nevertheless, the energy model is limited to the performance ratio calculation [21]. In [22], an in-situ calibration methodology for heterogeneous acquisition systems in PV plants is proposed. It introduces a multifunction calibrator for the traceable reference measurements of electrical signals, temperature, and irradiance, ensuring the measurement accuracy. Also in this case, the energy calculation is limited to the efficiency of the PV modules. A combination of PV modules modelling and measurement analysis is presented in [23], where the estimation of the required environmental quantities is analyzed together with their measurement system specifications.

Table I summarizes the review of energy modelling and measurements on PV modules. The 3<sup>rd</sup> column “energy modelling” includes paper with a detailed discussion of the energy model; the papers comparing theoretical models with measurements, without modifying model parameters, are in 4<sup>th</sup> column. If the model parameters are changed to match the measurements, the reference is listed in the 5<sup>th</sup> column.

TABLE I. REVIEW ON ENERGY MODELLING AND MEASUREMENTS ON PV MODULES AND ARRAYS

Reference	Monitoring system description, calibration, and uncertainty	Energy estimation	Energy modelling	between measurements and ex	Ex post optimization of the model
[8]			X	X	X
[9]			X	X	
[10]	X	X	X	X	
[11]			X	X	
[12]			X	X	
[13]			X	X	
[14]			X	X	
[15]			X	X	
[16]			X	X	
[17]	X			X	
[18]			X	X	
[19]			X	X	X
[20]	X	X		X	

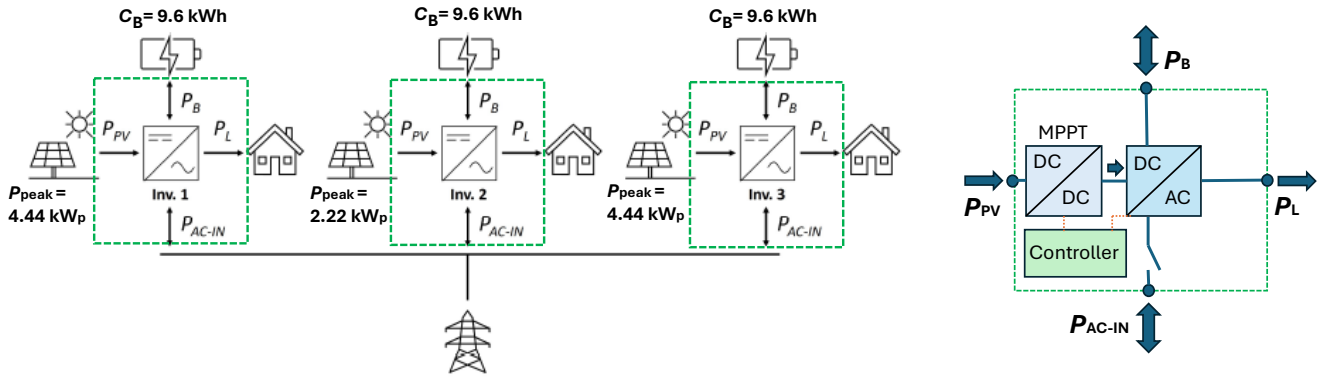


Fig. 1. The architecture of the PVZEN laboratory (left side), and internal block diagram of the converters (right side).

[21]	X	X		X	
[22]	X	X		X	
[23]	X		X	X	X

Regarding the modelling of DC/AC converters and electrochemical batteries in PV plants, the literature review highlights again that papers generally do not provide enough information about measurement systems and uncertainties [24]. Regarding the inverter efficiency calculation, the possible models for the conversion losses are generally polynomial functions [25] and the use of second-order polynomials is usually the compromise solution. In [26], the authors use the same model of [25] and propose a procedure to check the correct operation of the PV converter for losses estimation; in this case, the measurement uncertainty is provided. Another work providing details about measurements on PV converters is [27], in which efficiency measurements are performed both by electrical input-output and calorimetric methods for thermal losses.

Regarding the modelling of electrochemical batteries, circuit-based models are several [28]: the simplest one includes an ideal voltage source with an internal resistance, while more advanced versions integrate open circuit voltage, resistances, and RC circuits, with parameters identified through impedance spectroscopy techniques [29]. Mathematical models describe battery behavior using equations that relate physical quantities to internal circuit parameters, which are applicable to both charging and discharging conditions [30]. Nevertheless, in most cases, the papers provide information about measurement, but to perform them it is necessary to use small batteries, or in case of commercial devices, to open and disassemble the battery case, for example to disconnect the battery management system [31]. In this work, for the purpose of energy modelling, the State of Charge (SOC) model is selected for its simplicity, but adequate for microgrid energy modelling. It can be applied to any electrochemical storage device, and measurements can be easily performed on commercial systems.

### III. THE PVZEN PROJECT

The PVZEN project is based on an experimental laboratory for energy communities at the Politecnico di Torino campus [32]. The laboratory includes PV generators, electrochemical accumulators, and electric users, including heat pumps for air conditioning (heating/cooling) of lab rooms and generic appliances such as lamps and electronic devices. Since the PV power profiles differ from users' power profiles, electro-chemical storage systems give the possibility to compensate for this mismatch, permitting an optimal synergy between self-consumption of electrical production and self-sufficiency of users' consumption. The PVZEN laboratory enables the testing of both the off-grid operation and the energy-community operation for the users. The role of the external utility grid is to support the micro-grid in case of electricity production deficit, above all during winter season.

#### *A. Configuration of the PVZEN laboratory*

Fig. 1 (left side) shows the main components of the three users in the PVZEN laboratory, i.e., the PV generators, the storage systems and the DC/AC converters. The electronic converters, in which the main functions are represented in Fig. 1 (right side) as black boxes, are crucial devices for the correct operation of micro-grids, since thanks to a controller they provide:

- the internal MPP Tracker (MPPT) capability that optimizes the operation on the  $I-V$  curve of the PV generators by a DC-DC converter ( $P_{PV}$  in Fig. 1);
- the regulation of charge/discharge of the accumulators according to the constraints of their state of charge, but in the PVZEN lab the battery management systems are provided by the manufacturer of the lithium batteries ( $P_B$ );
- the suitable power quality (the output  $P_L$ ) in terms of frequency and Root Mean Square (RMS) value of the voltage waveform, minimizing the harmonic distortion in the DC-AC converter equipped with MOSFETs, commutated at 20 kHz by pulse width modulation; an internal switch enables or disables the connection to the external utility grid ( $P_{AC-IV}$  in Fig. 1).

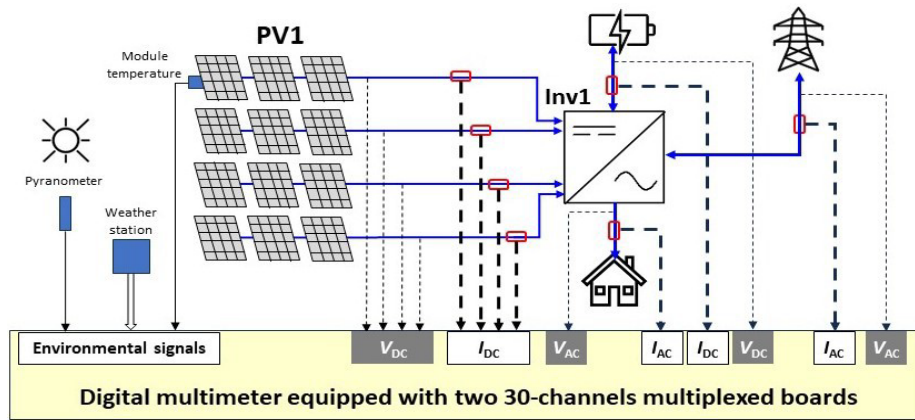


Fig. 2. Block scheme of the monitoring system installed on the first plant (PV generator with 12 modules) of the PVZEN laboratory.

The users are connected in parallel with each other as well as with the grid. Within this configuration, users can share their energy surplus with each other and can receive power from the external grid in case of energy deficit. The PV system is subdivided into three photovoltaic generators with a total peak power of 11.1 kWp (the peak power expressed in Wp refers to an irradiance value  $G_{STC} = 1000 \text{ W/m}^2$ ). The mono-crystalline silicon (m-Si) PV modules have a rated efficiency of 21.4 % and a peak power of 370 Wp. The PV-module orientation towards the South in the northern hemisphere, combined with a tilt angle that depends on the latitude, allows to maximize the energy production. Nevertheless, the PV arrays in PVZEN have been installed to represent different non-optimal installation conditions on the rooftops of apartment buildings, especially regarding the azimuth angles. The first PV generator is equipped with 12 modules (peak power of 4.44 kWp) with an orientation (SE) of  $-64^\circ$  relative to South ( $-90^\circ$  is East,  $0^\circ$  is South and  $90^\circ$  is West). The second PV generator includes 6 modules (peak power of 2.22 kWp) with an orientation of  $116^\circ$  (NW). The third PV generator includes 12 modules (peak power of 4.44 kWp) that are subdivided into two 6-module sub-generators: the first one has an orientation of  $-64^\circ$  (SE) relative to South and the second one an orientation of  $116^\circ$  (NW) relative to South. All the PV modules have a tilt angle of about  $10^\circ$ . As a result of the non-optimal installation conditions, irradiance is always lower than  $1000 \text{ W/m}^2$ , then arrays never reach the peak power. For example, for the 4.44 kWp strings, the maximum power does not exceed 3.2 kW.

The storage systems of the three users exhibit equal energy capacities. Each user is equipped with four lithium batteries with a nominal energy capacity of 2.4 kWh per unit, thus obtaining a total nominal energy capacity of 9.6 kWh for each user and an overall capacity of 28.8 kWh for the microgrid. The batteries have a nominal voltage of 48 V, a charge capacity of 50 Ah, a maximum

charging and discharging current of 100 A for one minute, and a Depth Of Discharge (DOD) of 90%, thus the minimum SOC is 10%.

Regarding the DC/AC conversion with sinusoidal output voltage ( $230 V_{\text{rms}}$ , 50 Hz), each user is equipped with a 5 kW converter that is designed to work both grid-connected and off-grid. For this reason, each device has an AC input for the connection to the grid and an AC output for the connection to the loads. The block diagram on the right side of Fig. 1 shows the main components of the converter: the DC power from PV array can feed the storage system, permitting its charge: as previously written, this DC/DC converter is equipped with a MPPT. The DC/AC stage can work also receiving AC power from the utility grid to charge the lithium batteries at DC side (rectifier mode); then, the power injection into the grid is set to zero. The connection with the grid can be disconnected ( $P_{\text{AC-IN}}$ ) for off-grid operations.

Regarding the electrical loads, the three generation units are independently connected to real users, which are a laboratory of electronic measurements, some office appliances of a room, and a computer-server room. Moreover, each unit supplies a resistor bench that can reproduce known profiles of residential or office users, including heat pumps. The maximum power that each resistor can dissipate is 4 kW.

Each inverter is equipped with a control and monitoring device that provides real-time information on the status of both inverter and PV-storage system that is connected to the same inverter. The main measurements provided by the inverter include the PV power ( $P_{\text{PV}}$ ), the power exchanged with the storage system ( $P_{\text{B}}$ ), the power absorbed from the AC input ( $P_{\text{AC-IN}}$ ), and the power delivered to the load ( $P_{\text{L}}$ ). In addition, the inverter reports the State Of Charge (SOC), the charge/discharge voltage, and the temperature of the storage system. According to the manufacturer's specifications, the maximum relative admitted error for the measurements provided by the instrumentation built into the inverter is  $\pm 3\%$  ( $\pm 5\%$ ) for real-time measurements when the output power is higher (lower) than 20% of the rated power. One should note that the majority of manufacturers does not provide any information that allows the uncertainty of the measured quantities to be evaluated and the traceability of the same measurements is rarely ensured. For this reason, the monitoring system in PVZEN, which is described in section III-C, is a useful tool to obtain traceable measurements that are fully characterized in terms of uncertainty.

### *B. Theoretical models for the simulation of PVZEN equipment*

The PVZEN microgrid is based on PV generation and lithium batteries. This subsection presents the selected energy models available in the literature for PV modules, DC/AC converters and storage

systems. These models are selected because they offer a good tradeoff between accuracy and computational effort. Indeed, energy models employ equations to compute input/output efficiencies of energy transformations through the determination of the losses in the processes (they are optical in the glass of PV modules, electrical in the DC to AC conversion, etc.). However, energy models do not permit the reconstruction of waveforms (DC ones with ripples and AC ones with harmonics) and so the time scale is a minute or multiples of it, as a quarter of an hour. Moreover, the selected models can be easily included in convex or linear optimization [33], permitting easier and better management in case of steady-state simulation and control of a high number of users. The only model that cannot be totally linearized is the *SOC* calculation, because it includes an “if” condition, i.e., the formula changes whether the battery is in charge or in discharge state [34]. Moreover, the selected models can be used in most of the microgrid configurations and neither the selected energy models nor the proposed measurement procedures are affected by the interactions between users in the grid, particularly with regard to the converter and battery models.

To calculate the production of a PV system, the global irradiance  $G$  on the module plane and the air temperature  $T_{\text{air}}$  are required [35]. These quantities can be measured by a weather station near the PV system or downloaded from online services [36]. In this PVZEN lab, the global irradiance has been measured by a pyranometer placed on the horizontal plane and the experimental results have been corrected to represent the irradiance on the plane of PV modules by the conventional method [8]. However, this method exhibits poor accuracy at low irradiance levels ( $G < 300 \text{ W/m}^2$ ), as will be clarified in the Section VI.B, because diffuse irradiance is evaluated with an assumption of isotropic sky. As written in Section II, to evaluate the electrical power generated by PV modules ( $P_{\text{PV}}$ ), a “DC model” is used according to the following equations:

$$P_{\text{PV}} = P_{\text{peak}} \cdot (G / G_{\text{STC}}) \cdot \eta_{\text{lowG}} \cdot \eta_{\text{temp}} \cdot \eta_{\text{mix}} \quad (1)$$

$$\eta_{\text{temp}} = 1 + \gamma_{\text{th}} \cdot (T_{\text{mod}} - T_{\text{mod,STC}}); \quad \eta_{\text{lowG}} = 1 - (G_0 / G) \quad (2)$$

- $P_{\text{peak}}$  is the peak (or rated) power of the PV system at Standard Test Conditions (STC), i.e., irradiance  $G_{\text{STC}} = 1 \text{ kW/m}^2$  and module temperature  $T_{\text{mod,STC}} = 25 \text{ }^\circ\text{C}$ ;
- $G_0$  is the irradiance threshold value below which there is no PV generation in this hyperbolic model;
- $\gamma_{\text{th}}$  is the coefficient that expresses the dependence of the PV generation on module temperature  $T_{\text{mod}}$ ;
- $\eta_{\text{mix}}$  is the mixed efficiency, which takes into account several loss factors, such as reflection and refraction losses, module soiling, mismatch losses and losses in cables due to Joule effect.

The module temperature is evaluated from  $T_{\text{air}}$  and  $G$  using the following equation:

$$T_{\text{mod}} = T_{\text{air}} + (\text{NOCT} - T_{\text{air,NOCT}}) \cdot (G / G_{\text{NOCT}}) \quad (3)$$

where NOCT is the Nominal Operating Cell Temperature, which is the module temperature when the air temperature  $T_{\text{air,NOCT}} = 20 \text{ }^\circ\text{C}$ , the irradiance  $G_{\text{NOCT}} = 800 \text{ W/m}^2$  and the wind speed is  $1 \text{ m/s}$  [37].

Regarding the DC/AC converters, power conversion losses  $P_{\text{losses}}$  can be modelled as a function of the output power  $P_{\text{out}}$  using the following quadratic equation:

$$P_{\text{losses}} = k_{\text{quad}} \cdot (P_{\text{out}})^2 + k_{\text{lin}} \cdot P_{\text{out}} + P_0 \quad (4)$$

where  $k_{\text{quad}}$  models the losses as a square function of  $P_{\text{out}}$  and  $k_{\text{lin}}$  represents the losses linearly proportional to  $P_{\text{out}}$  and  $P_0$  is the converter self-consumption power [38].

The operation of a storage system can be described by the evolution of its State Of Charge (SOC), which is defined as the ratio of residual to nominal energy capacity [39]. The SOC at the time instant  $t$  can be evaluated from the SOC at the previous time instant ( $t - 1$ ) using the following equations for the charge and discharge phase, respectively:

$$\text{SOC}(t) = \text{SOC}(t - 1) + \frac{|P_B| \cdot \Delta t \cdot \eta_{\text{ch}}}{C_B} - \frac{P_{\text{self-disch}} \cdot \Delta t}{C_B} \quad (5)$$

$$\text{SOC}(t) = \text{SOC}(t - 1) - \frac{|P_B| \cdot \Delta t}{C_B \cdot \eta_{\text{disch}}} - \frac{P_{\text{self-disch}} \cdot \Delta t}{C_B} \quad (6)$$

- $P_B$  is the charge/discharge power in the time interval  $\Delta t$ ;
- $C_B$  is the nominal energy capacity of the storage system;
- $\eta_{\text{ch}}$  and  $\eta_{\text{disch}}$  are the charge and discharge efficiencies;
- $P_{\text{self-disch}}$  is the self-discharged power.

### C. The monitoring system

The measurement of time-variant electrical quantities can be carried out with two techniques: one is the multimeter approach, in which the RMS values of voltage and current waveforms and the average value of instantaneous power (active power) are the most important goals (high number of bits to obtain good resolution); the other one is the oscilloscope approach, in which the correct definition of the waveforms is the most important output (high sampling rate but poor resolution).

For the commercial electronic converters, the multimeter approach is chosen by the manufacturers of a DC-DC converter and a DC-AC converter, to give general information about the input/output performance. Hence, also the instrumentation, used as a reference system by the authors, has the

same multimeter approach, but with higher number of bits in terms of resolution to ensure better accuracy.

The models described in Section III-B, which allow the behavior of PV generators, DC/AC converters and storage systems to be evaluated, can be identified using the measurements provided by the devices embedded in the inverters. However, equations (1) and (3) also require environmental quantities, such as the irradiance on the plane of the PV modules and the air temperature, which are not usually available. In addition, the traceability of the measurements of the electrical quantities provided by the inverters is not ensured and the uncertainty of these measurements is rarely stated. To fill this gap, the PVZEN laboratory has been equipped with a monitoring system that is able to measure both electrical and environmental quantities. Such a system is subjected to metrological confirmation [40], thus ensuring the traceability requirement and providing a full characterization of the different measuring chains in terms of uncertainty.

A block scheme of the monitoring system that has been installed at the PVZEN laboratory is shown in Fig. 2, which refers to the first plant (PV generator with 12 modules). The other two plants are monitored in the same way for the DC and AC electrical quantities, while the environmental quantities are measured by a single pyranometer and a single weather station. The monitoring system is based on a 7 and half digits multimeter that embeds two 30-channels insulated multiplexed boards. The DC and AC voltages are directly connected to one board (gray background color in the figure), while the other low-level analog signals are connected to the second board (white background color in the figure).

About the PV generator, the DC voltage ( $V_{dc}$ ) of each string made up of 3 modules is measured (thin dashed lines in Fig. 2) as well as the current of each string ( $I_{dc}$ ), which is converted into a voltage signal (thick dashed lines in Fig. 2) by means of a through-hole sensor with range of 50 A, nominal conversion factor of 40 mV/A and uncertainty stated as  $\pm(0.05\% \cdot reading + 0.01\% \cdot range)$  A. The DC voltage of the storage system is also measured and the corresponding current is sensed through a through-hole sensor with range of 500 A, nominal conversion factor of 4 mV/A and uncertainty stated as  $\pm(0.04\% \cdot reading + 0.008\% \cdot range)$  A.

For the AC quantities, the inverter is monitored both on the input (mains) and output (load) sides. The voltage lines are directly routed to the same board that measures the DC voltages, while the current from the mains and the current to the load are converted to voltage signals by means of clamp meters with ranges of 20 A and 200 A, nominal conversion factors of 100 mV/A (range 20 A) and 10 mV/A (range 200 A), bandwidth of 1 kHz and uncertainty stated as  $\pm(1.5\% \cdot reading + 0.5)$  A. The

monitoring system provides the active power  $P_{AC}$  with a relative uncertainty of  $\pm 0.2\%$  in the range (0.1 ÷ 5) kW.

Solar irradiance is measured on the horizontal plane by means of a broadband secondary-standard pyranometer with a nominal sensitivity of  $10 \mu V/W/m^2$ . The voltage signal at the output of the pyranometer, which exhibits maximum values of about 10 mV, is amplified (nominal gain 100) and then connected to an input channel of the multiplexed board that collects all the low-level analog signals. The relative measurement uncertainty of the solar irradiance is 2%, which mainly depends on the instrumental uncertainty of the pyranometer and its calibration uncertainty.

The board that measures the pyranometer output also receives the signals from a device that senses the temperature of a module of the PV generator and from a weather station, which provides the measurement of the quantities:

- air temperature and relative humidity, uncertainty  $\pm 0.5$  °C in the range (−20 ÷ 60) °C and  $\pm 3$  %UR in the range (10 ÷ 90) %UR, respectively;
- wind speed and direction, uncertainty  $\pm 0.5$  m/s in the range (1 ÷ 40) m/s and  $\pm 5$  ° in the range (0 ÷ 360) °, respectively;
- atmospheric pressure, and precipitation absence/presence.

#### IV. CHARACTERIZATION OF THE MONITORING SYSTEM

Before the installation of the monitoring system in the PVZEN laboratory, all the measurement chains that are not provided with a calibration certificate have been subjected to a preliminary metrological characterization against reference standards (multifunction calibrator, digital multimeter and wattmeter). Such a characterization, which has been performed at the Testing and Calibration Laboratory of the Electronics and Telecommunications Department of Politecnico di Torino, has involved the digital multimeter and the DC and AC current sensors described in the previous section. During the characterization, the multimeter of the monitoring system has been set in the same configuration as it is used in the PVZEN laboratory, using an integration interval of 1 PLC to ensure a suitable noise rejection.

About the measurement of DC and AC voltages, the multimeter exhibited measurement errors that were compliant to its specifications, then the instrumental uncertainty for these quantities is  $(0.005\% \cdot \text{reading} + 0.003)$  V in the range 300 V for DC voltage measurements and  $(0.06\% \cdot \text{reading} + 0.15)$  V in the range 300 V and in the frequency range (0.04 ÷ 20) kHz for AC voltage measurements.

Also, for the measurement chains of DC currents, which include the multimeter and the through-hole current sensors, and AC currents, which include the multimeter and the clamp meters, measurement errors during the characterization resulted compliant to the maximum admitted errors obtained by the combination of the specifications of multimeter and current sensors. The corresponding instrumental measurement uncertainty is then  $(0.1\% \cdot \text{reading} + 0.01)$  A in the range 50 A (DC current measurements of the PV strings);  $(0.5\% \cdot \text{reading} + 0.5)$  A in the range 500 A (DC current measurements of the storage systems);  $\pm(2.0\% \cdot \text{reading} + 0.2)$  A in the range  $(0.5 \div 20)$  A and in the frequency range  $(0.04 \div 1)$  kHz (AC current measurements).

For the measurement of AC active power, the multimeter was compliant to its specifications, then the instrumental relative uncertainty for this quantity is 0.2% in the range  $(0.1 \div 5)$  kW and in the frequency range  $(0.04 \div 1)$  kHz.

## V. METHODOLOGY FOR MODELS OPTIMIZATION

The parameters involved in the models described in section III-B were identified starting from environmental and electrical measurement data. In the following subsections, the procedures for estimating the parameters are described.

### A. PV generator

In equation (1),  $P_{\text{nom}}$  and  $\gamma_{\text{th}}$  are provided by the manufacturer, while  $\eta_{\text{mix}}$  and  $G_0$  have been estimated. For the evaluation of the parameters, the measured PV power ( $P_{\text{PV\_meas}}$ ) was compared to the estimated value obtained from equation (1). In particular, the parameters resulted from the minimization of the square error between the measured power and its prediction considering  $N$  sets of input data (i.e., sets containing module temperature  $T_{\text{mod\_meas}}$  and irradiance  $G_{\text{meas}}$  values sampled at the same time). The mathematical formulation of the optimization problem is the following:

$$\min_{G_0, \eta_{\text{mix}}} \sum_i^N [f(G_0, \eta_{\text{mix}}, G_{\text{meas},i}, T_{\text{mod\_meas},i}) - P_{\text{PV\_meas},i}]^2 \quad (7)$$

where  $f$  is equation (1) with the parameters  $\gamma_{\text{th}} = -0.003 \text{ } ^\circ\text{C}^{-1}$  and  $P_{\text{nom}}$  equal to the rated power of each PV generator.

The parameter optimization was carried out for all different string orientations of each PV generator. Therefore, one set of parameters was determined for generator #1 ( $P_{\text{nom}} = 4.44$  kW) and another one for generator #2 ( $P_{\text{nom}} = 2.22$  kW). On the contrary, two sets were identified for generator #3 ( $P_{\text{nom}} = 2.22$  kW for each orientation). The optimization was carried out using the trust-region-reflective algorithm.

Regarding the module temperature, the *NOCT* is the parameter to be estimated in equation (3). In this case, the measured module temperature  $T_{mod\_meas}$  was compared to the estimated value, according to the following formula:

$$\min_{NOCT} \sum_i^N [g(NOCT, G_{meas,i}, T_{air\_meas,i}) - T_{mod\_meas,i}]^2 \quad (8)$$

where  $g$  is equation (3). The input data for equation (3) were the measured air temperature ( $T_{air\_meas}$ ) and the measured irradiance on the module plane ( $G_{meas}$ ). Since the module temperature is measured on the rear surface of the central modules of four strings (1E, 2W, 4W and 6E), two for each orientation, four separate optimizations were carried out. The same algorithm employed for the evaluation of  $G_0$  and  $\eta_{mix}$  (trust-region-reflective algorithm) was used.

### *B. Inverter*

From the power conversion loss formulation in equation (4), the inverter input power ( $P_{in}$ ) can be expressed as:

$$P_{in} = P_{out} + P_{losses} = K_0 \cdot P_{nom} + (K_1 + 1) \cdot P_{out} + \frac{K_2}{P_{nom}} \cdot P_{out}^2 \quad (9)$$

where  $P_{nom}$  is the inverter nominal power,  $K_0$  is equal to  $P_0/P_{nom}$ ,  $K_1$  is equal to  $k_{in}$  and  $K_2$  is equal to  $k_{quad} \cdot P_{nom}$ . The three parameters  $K_0$ ,  $K_1$  and  $K_2$  were estimated. Since the PVZEN inverters are bi-directional, two sets of parameters were determined, one for DC/AC conversion and another one for AC/DC conversion. For evaluating each set of parameters, the power entering ( $P_{in\_meas}$ ) and the power exiting the inverter ( $P_{out\_meas}$ ) measured by the data logging device of the inverters were used. The parameters resulted from minimizing the square error between the measured input power and its prediction, calculated using equation (9). The mathematical formulation of the optimization problem is the following:

$$\min_{K_0, K_1, K_2} \sum_i^N [h(K_0, K_1, K_2, P_{out\_meas,i}) - P_{in\_meas,i}]^2 \quad (10)$$

where  $h$  is equation (9) with  $P_{nom}$  equal to 5 kW in DC/AC conversion and 3.5 kW in AC/DC conversion. Also in this case, the optimizations were performed in MATLAB using the trust-region-reflective algorithm.

#### A. Storage system

Three parameters associated with the selected *SOC* model need to be defined: charge and discharge efficiencies and self-discharge power. For the estimation of  $\eta_{ch}$ ,  $\eta_{disch}$  and  $P_{self-disch}$ , the

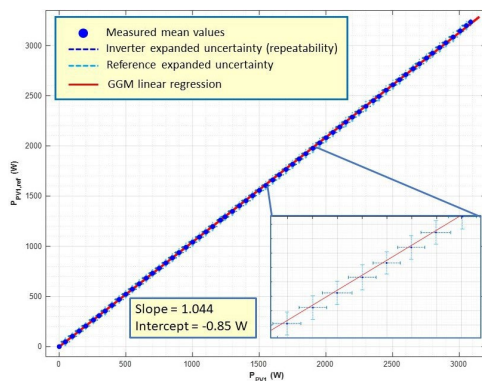


Fig. 3. Generalised Gauss-Markov linear regression among the power measurements related to the PV generator of the first plant of the PVZEN laboratory.

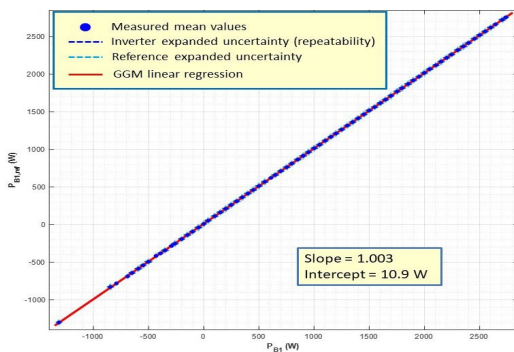


Fig. 4. Generalised Gauss-Markov linear regression among the power measurements related to the storage system of the first plant of the PVZEN laboratory

charging and discharging power  $P_B$  was needed together with the  $SOC$  evolution. Indeed, the predicted  $SOC$ , evaluated using equations (5) and (6), was compared to the  $SOC$  value provided by the battery management system through the data logging device of the inverter. Regarding  $P_B$ , it was calculated from the voltage and current measurements performed by the PVZEN monitoring system. The three parameters resulted from minimizing the square error between the measured  $SOC$  and its prediction. The mathematical formulation of the minimization problem is the following:

$$\min_{\substack{\eta_{ch}, \eta_{disch}, \\ P_{self-disch}}} \sum_i^N [m(\eta_{ch}, \eta_{disch}, P_{self-disch}, P_{B_{meas,i}}, \Delta t_i) - SOC_{meas,i}]^2 \quad (11)$$

where  $m$  is equation (5) in charging and equation (6) in discharging, with  $C_B$  equal to 9.6 kWh. In this case, the  $N$  pairs of input measured data must be time-consecutive because the  $SOC$  of a given moment depends on the previous one. In the first analyzed instant, the  $SOC$  of the previous interval was set equal to the measured one. The optimizations were carried out using the trust-region-reflective algorithm.

## VI. RESULTS

### A. Evaluation of Measurement Errors

One of the main outcomes of the monitoring system is the evaluation of the measurement errors of the devices internal to the inverters of the PVZEN laboratory that provide DC power ( $P_{PV}$  and  $P_B$ ) and AC power ( $P_L$  and  $P_{AC-IN}$ ). The identification of the models described by the equations (1), (4), (5) and (6) can take advantage from this kind of characterization. Furthermore, the comparison among the identification results based on the power measurements provided by the inverters and the ones obtained using the power measurements of the monitoring system is of great interest. The first comparison has involved the measurements of the DC power provided by the three PV generator of the PVZEN laboratory ( $P_{PV1}$ ,  $P_{PV2}$  and  $P_{PV3}$ ) and the measurements of the power exchanged between inverters and storage systems ( $P_{B1}$ ,  $P_{B2}$ , and  $P_{B3}$ ). These quantities are compared to the power measurements provided by the monitoring system, which are obtained as the product between each DC voltage and the corresponding DC current, thus obtaining the reference values  $P_{PV_i,ref} = V_{PV_i,ref} \cdot I_{PV_i,ref}$  and  $P_{PB_i,ref} = V_{Bi,ref} \cdot I_{Bi,ref}$  ( $i = 1, 2, 3$ ).

Since the measurement devices embedded into the inverters are not synchronous with respect to the monitoring system, a specific pre-processing has been implemented in order to align the available results. In addition, the inverters have an update rate of 1 min (average of 12 samples with 5 s acquisition interval), while the digital multimeter of the monitoring system updates the reference values with an interval of 20 s. For this reason, the comparison has been

made among the average values provided by the inverters and the 4-sample moving average of reference values of the multimeter, thus covering a common time interval of 1 min. The measurements acquired from November 2022 to May 2023 have been processed selecting days characterized by clear weather conditions. The range of power measurements  $P_{PVi}$  and  $P_{Bi}$  provided by the inverters have been subdivided into equally spaced intervals and the corresponding measurements  $P_{PVi,ref}$  and  $P_{Bi,ref}$  have been associated to each interval. The mean value and the experimental standard deviation (type-A method for uncertainty evaluation according to the GUM approach [41]) of each quantity have been evaluated for each sub-interval and an unweighted least-square method has been implemented to obtain a preliminary linear fitting of the power mean values. Then, an outlier removal technique has been implemented that is based on the standard deviation  $\sigma_{res}$  of the regression residuals, excluding measurements that provide residuals that exceed  $3 \cdot \sigma_{res}$ . Once the complete dataset has been obtained, a Generalised Gauss-Markov (GGM) linear regression [42] has been used to relate the power measurements provided by the inverters to the corresponding measurements from the monitoring system.

The linear regression results referring to the first PV generator are reported in Fig. 3 in the range of about 0 W to 3.2 kW. In the figure, the blue dots are the couples of mean values  $P_{PV1}/P_{PV1,ref}$  obtained with the procedure described above, while the red line is the result of the GGM linear regression, which takes into account both the uncertainty of reference values (instrumental uncertainty + noise, light blue dashed lines in the figure) and reading of the inverter (noise, dark blue dashed lines in the figure). The main outcome of this analysis is the estimation of gain and offset errors of the device internal to the inverter, which are  $-4.4\%$  and  $+0.85$  W.

The same results referring to the storage system of the first plant of the PVZEN laboratory are reported in Fig. 4 in the range of about  $-1.3$  kW to  $2.7$  kW, where the minus sign is related to a power exchange from the battery to the inverter. In this case, the device internal to the inverter has shown a gain error of  $-0.3\%$  and an offset error of about  $-11$  W.

Similar results have been obtained for the other two sections of the PVZEN laboratory, as summarized below:

- $P_{PV2}$ : gain error =  $-4.6\%$ , offset error =  $1.5$  W;
- $P_{PV3}$ : gain error =  $-4.3\%$ , offset error =  $0.5$  W;
- $P_{PB2}$ : gain error =  $-0.1\%$ , offset error =  $-13$  W;
- $P_{PB3}$ : gain error =  $-0.5\%$ , offset error =  $-8$  W.

## B. Models optimization

The following subsections show the results of the optimization processes carried out to evaluate the parameters involved in the energy models. These results are obtained by averaging 1-min profiles to obtain 15-min profiles. This averaging is done to mitigate the lower performance observed in the measurement of irradiance values lower than  $300 \text{ W/m}^2$ , even though a second-class pyranometer is employed. This approach is justified by the purpose of the present work; actually, according to [43] the energy flows in grid applications are mostly calculated with quarter-hourly data.

1) *PV generator*: The obtained values for  $G_0$  and  $\eta_{\text{mix}}$  are shown in Table II, where the parameter  $G_0$  is included in a narrow range from  $24 \text{ W/m}^2$  to  $27 \text{ W/m}^2$ , while the parameter  $\eta_{\text{mix}}$  has values between 0.84 and 0.91. The deviation of  $\eta_{\text{mix}}$  is mainly due to the PV module orientation between SE and NW, which can be due to different optical losses (reflection and refraction). Indeed, the PV strings with the same orientation show similar efficiencies. The analysis of the results that refer to the PV power calculated by equation (1) with respect to the PV power measured by the monitoring system highlights large deviations in the low power range, i.e. for power lower than 1 kW, as evident in Fig. 5. The main reasons for this behavior are: the use of the simplest model for the low irradiance-losses [44]; the poor MPPT capability at irradiance lower than  $300 \text{ W/m}^2$ ; the high uncertainty of the indirect measurements provided by the irradiance sensor in the above mentioned irradiance range.

Table III displays some results that were obtained using  $N \approx 7700$  data points, corresponding to about 1900 h of operation. The squared error appearing in the objective function to be minimized is expressed through the square root of its mean value, referred to as Root Mean Square Error (*RMSE*):

$$RMSE = \sqrt{\sum_{i=1}^n \frac{(\hat{y}_i - y_i)^2}{n}} \quad (12)$$

where  $\hat{y}_i$  is the predicted value,  $y_i$  is the measurement, and  $n$  is the number of observations. The *RMSE* is reduced during the process as well as the difference between the PV energy calculated using the measured power and the PV energy calculated considering the power estimated with equation (1). In particular, the energy difference becomes lower than 1%, in absolute value, for each PV generator.

TABLE II

$G_0$  AND  $\eta_{\text{mix}}$  ESTIMATED VALUES.

PV generator (orientation)	$G_0$ (W/m <sup>2</sup> )	$\eta_{\text{mix}}$ (-)
#1 (SE)	24	0.91
#2 (NW)	27	0.84
#3 (SE)	25	0.89

To improve the model behavior at low power level, another model for low-irradiance losses is adopted, that is based on the following expression of the parameter  $\eta_{\text{lowG}}$ :

$$\eta_{\text{lowG}} = 1 - e^{(-G / G_0)} \quad (13)$$

The model identification with the equation (13) for  $\eta_{\text{lowG}}$  provided the results reported in Fig. 6 for the first PV generator, where the optimization process brings to the new parameters  $G_0 = 91$  W/m<sup>2</sup> and  $\eta_{\text{mix}} = 0.87$ . This exponential model for  $P_{\text{PV calc}}$  is very close to the hyperbolic model, since the slopes of the fitted curves are both higher than 0.98 and the constant terms are lower than 0.01, where the first is negative and the second positive. The future upgrade to reduce these remarkable deviations with power levels lower than 1 kW will be the installation of an irradiance sensor, based on a calibrated solar cell, on the plane of the PV modules.

2) *Inverter*: In Table IV the two sets of parameters involved in the conversion power loss model are

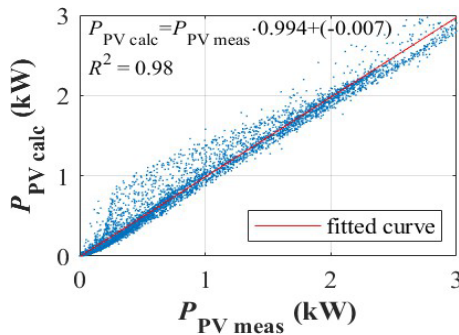


Fig. 5. Identification results of PV generator model using the hyperbolic expression for the parameter  $\eta_{\text{lowG}}$ .

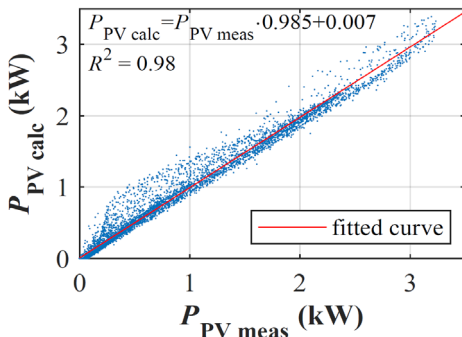


Fig. 6. Identification results of PV generator model using the exponential expression for the parameter  $\eta_{\text{lowG}}$ .

shown, together with additional details about the optimization results. The subscript "in" refers to "initial" condition; thus, it is used for inputs parameters from literature (for example,  $G_{0,in}$  and  $\eta_{mix,in}$ ). The subscript "in" is also used to identify the results of the mathematical model before optimization, i.e. the models with initial parameters. The implemented optimization reduced the initial  $RMSE$  ( $RMSE_{in}$ ), showing that the obtained parameters can represent the conversion losses better than their assumed initial values. These results represent a preliminary estimation as they were evaluated using measurements provided by the inverters, which are based on low-accuracy multi-meter. Improvements are expected in future work using measurements acquired by certified instruments.

3) *Storage system*: The values of the parameters obtained for the three storage systems are shown in Table V. The  $RMSE$  between the measured  $SOC$  and its prediction is reduced to a few percentage points using the identified parameters ( $RMSE_{opt}$ ). Similar results were obtained for the three systems: this is reasonable as they consist of the same number of battery modules, are operated by the same type of battery management system and connected to an inverter of the same model, and were installed on the same date, which means same ageing. The charge and discharge efficiencies resulted in 98%. The average self-discharge power is 6 W, confirming a low value for lithium batteries. Using the identified parameters, the prediction of the SOC is close to that measured, as shown in Fig. 7 for the BESS #3.

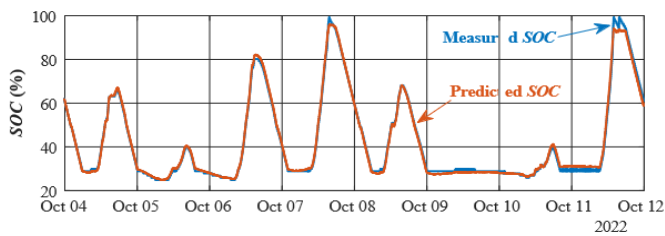


Fig. 7. Measured (blue line) and predicted (red line)  $SOC$  for the BESS #3.

TABLE III

RMSE AND ENERGY DIFFERENCE BETWEEN MEASUREMENTS AND PREDICTIONS.

PV generator (orientation)	Using $G_{0,in}$ and $\eta_{mix,in}$		Using $G_0$ and $\eta_{mix}$	
	RMSE (W)	Energy difference	RMSE (W)	Energy difference
#1 (SE)	106.9	3.3%	103.2	-0.39%
#2 (NW)	81.7	13.3%	61.8	0.56%
#3 (SE)	61.4	5.5%	56.4	-0.24%
#3 (NW)	70.5	11.9%	53.1	-0.23%

TABLE IV

RESULTS OF INVERTER PARAMETERS EVALUATION.

Direction	$RMSE_{in}(W)$	$RMSE_{opt}(W)$	$K_0$	$K_1$	$K_2$

DC/AC	50.6	42.5	0.014	0.008	0.153
AC/DC	44.0	25.6	0.020	0.005	0.165

TABLE V

RESULTS OF STORAGE SYSTEM PARAMETERS EVALUATION.

BESS	$RMSE_{in}(\%)$	$RMSE_{opt}(\%)$	$\eta_{ch}$	$\eta_{disch}$	$P_{self-isch} (W)$
#1	40	2.0	0.98	0.98	2.9
#2	28	2.5	0.98	0.98	8.6
#3	35	1.2	0.98	0.98	6.1

## VII. CONCLUSIONS

A methodology has been proposed in this paper for identifying reliable models that describe the behavior of the components of a PV plant, which are PV generators, power converters and storage systems. Results that refer to the identification of these models for the components of the PVZEN laboratory have been also reported, which could enable other researchers in simulating energy communities in different climate conditions and with different load profiles. Particular attention has been paid towards the reliability of the identified models, which is strongly related to the measurements of the involved quantities, which are DC and AC power and environmental quantities. With the aim of obtaining traceable measurements that are qualified in terms of uncertainty, a monitoring system has been installed along the whole PVZEN laboratory that is able to provide environmental quantities and electrical quantities upstream and downstream the power converters.

Experimental results are provided that refer to the characterization of the measuring devices embedded into the inverters of the PVZEN laboratory as well as to the identification of the proposed models.

About the characterization step that refers to the measurement of the DC input power from the PV generators, negligible offset errors were obtained, while the gain errors were close to  $-5\%$  that exceed the manufacturer's specification (relative error of  $\pm 3\%$  for power measurements higher than  $20\%$  of the rated power). On the contrary, gain errors lower than  $-0.5\%$  and then compliant to the manufacturer's specifications were obtained for the measurement of the power exchanged between inverters and storage systems, with a maximum offset error of  $-13 W$ . These outcomes highlight the large difference between the uncertainty provided by the monitoring system installed along the PVZEN laboratory (see section III.C) and the uncertainty of the inverter measuring devices. For this reason, the models for PV generators and storage systems have been identified based on the monitoring-system measurements, which also ensure the metrological traceability. The identification process provided reliable models for the PV generators that exhibit root means square errors

between measured and predicted energy lower than 1 % during a time interval of about three months. Furthermore, the model at low irradiance values has been improved by means of an exponential relationship. About the storage systems, charge and discharge efficiency of 98 % have been obtained and the average self-discharge power for the three plants was of about 6 W, which is conform to the typical behavior of lithium batteries. For the models of the power inverters, the identification process relied on the AC power measurements provided by the measuring devices internal to the inverters, since the metrological characterization of these devices for AC measurements have not been completed yet. The preliminary results have shown the effectiveness of the optimization process, which allows the root mean square error of the power losses to be significantly reduced. However, better results are expected once the same models will be identified using the AC measurements provided by the reference monitoring system.

## REFERENCES

- [1] Directive (EU) 2018/2001 of the European Parliament and of the Council of 11 December 2018 on the promotion of the use of energy from renewable sources (recast).
- [2] Directive (EU) 2019/944 of the European Parliament and of the Council of 5 June 2019 on common rules for the internal market for electricity and amending Directive 2012/27/EU (recast).
- [3] A. Wierling et al. "A Europe-wide inventory of citizen-led energy action with data from 29 countries and over 10000 initiatives," *Scientific Data*, vol. 10, no. 9, 2023.
- [4] "Energy supply to the energy self-sufficient village of Feldheim via private local heating and electricity grids." Available online: <https://nef-feldheim.info/energieautarkes-dorf/> (access. Dec. 1, 2023).
- [5] "Samsø: An Island Community Pointing to the Future Denmark." Available online: <https://unfccc.int/climate-action/un-global-climate-action-awards/climate-leaders/> (access. Dec. 1, 2023).
- [6] "Salina-Isola pilota dell'UE." Available online: <https://www.fficienzaenergetica.enea.it/vi-segnaliamo/salina-isola-pilota-dell-ue.html> (Italian language, accessed Dec. 1, 2023).
- [7] A. Amato, A. Carullo, A. Ciocia, S. Corbellini, F. Spertino, A. Vallan, M.A.A. Bertolasco, "The PVZEN Laboratory for Energy Communities: Monitoring System for Model Identification," 2024 IEEE International Instrumentation and Measurement Technology Conference (I2MTC), Glasgow, United Kingdom, pp. 1-6, 2024.
- [8] A. Ciocia, G. Chicco and F. Spertino, "An Improved Model for AC Power From Grid Connected Photovoltaic Systems and Comparison With Large-Scale Hourly Measured Data," in *IEEE Transactions on Industry Applications*, vol. 60, no. 3, pp. 4458-4469, May-June 2024.
- [9] Milosavljević, D., Kevkić, T., e Jovanović, S. (2022). "Review and validation of photovoltaic solar simulation tools/software based on case study." *Open Physics*, 20(1), 431–451.
- [10] M. Fuentes *et al.*, "Application and validation of algebraic methods to predict the behaviour of crystalline silicon PV modules in Mediterranean climates," *Solar Energy*, vol. 81, 2007, pp.1396-1408.
- [11] J. Park *et al.*, "A probabilistic reliability evaluation of a power system including Solar/Photovoltaic cell generator," *IEEE Power and Energy Society General Meeting-PES'09*, pp. 1–6, 2009.

- [12] C.R., Osterwald, "Translation of device performance measurements to reference conditions," *Solar Cells*, vol. 18, pp. 269–279, 1996.
- [13] Humada, Ali M., Mojgan Hojabri, Saad Mekhilef, and Hussein M. Hamada. "Solar cell parameters extraction based on single and double-diode models: A review." *Renewable and Sustainable Energy Reviews*, vol. 56, pp. 494-509, 2016.
- [14] S. Prakash *et al.*, "Modeling and Performance Analysis of Simplified Three-Diode Photovoltaic Module." *Journal of Electrical Engineering* vol. 1, pp. 55-64, 2022.
- [15] A. Kumar and R. Agarwal, "Mathematical Modeling and Analysis of Single-Diode, Double-Diode and Triple Diode based PV Module," *2023 Intern. Conference for Advancement in Technology (ICONAT)*, Goa, India, pp. 1-6, 2023.
- [16] E. Bompard *et al.*, "Assessing the role of fluctuating renewables in energy transition: Methodologies and tools," *Applied Energy*, vol. 314, 2022.
- [17] C. Nemes and F. Munteanu, "An analysis of a photovoltaic panel model: Comparison between measurements and analytical models," *2012 International Conference and Exposition on Electrical and Power Engineering*, Iasi, Romania, 2012, pp. 939-944.
- [18] W. De Soto, S. A. Klein, and W. A. Beckman, "Improvement and validation of a model for photovoltaic array performance," *Solar Energy*, vol. 80, no. 1, pp. 78–88, 2006.
- [19] D. L. King, J. A. Kratochvil, and W. E. Boyson, *Photovoltaic Array Performance Model*, Sandia National Laboratories, Albuquerque, NM, Rep. SAND2004-3535, Aug. 2004. [Online]. Available: [https://energy.sandia.gov/wp-content/gallery/uploads/SAND-2004\\_PV-Performance-Array-Model.pdf](https://energy.sandia.gov/wp-content/gallery/uploads/SAND-2004_PV-Performance-Array-Model.pdf)
- [20] A. Carullo, S. Corbellini, A. Luoni and A. Neri, "In Situ Calibration of Heterogeneous Acquisition Systems: The Monitoring System of a Photovoltaic Plant," in *IEEE Transactions on Instrumentation and Measurement*, vol. 59, no. 5, pp. 1098-1103, May 2010.
- [21] A. Carullo and A. Vallan, "Outdoor Experimental Laboratory for Long-Term Estimation of Photovoltaic-Plant Performance," in *IEEE Transactions on Instrumentation and Measurement*, vol. 61, no. 5, pp. 1307-1314, May 2012.
- [22] F. J. Sánchez-Pacheco, P. J. Sotorriío-Ruiz, J. R. Heredia-Larrubia, F. Pérez-Hidalgo and M. S. de Cardona, "PLC-Based PV Plants Smart Monitoring System: Field Measurements and Uncertainty Estimation," in *IEEE Transactions on Instrumentation and Measurement*, vol. 63, no. 9, pp. 2215-2222, Sept. 2014.
- [23] L. Cristaldi, M. Faifer, M. Rossi and F. Ponci, "A Simple Photovoltaic Panel Model: Characterization Procedure and Evaluation of the Role of Environmental Measurements," in *IEEE Trans. on Instrumentation and Measurement*, vol. 61, no. 10, pp. 2632-2641, Oct. 2012.
- [24] X. Zhang, X. Zhang, S. Yang, X. Su, G. Liu, and L. Ma, "A review on energy, environment and economic assessment in remanufacturing based on life cycle assessment method," *Renewable and Sustainable Energy Reviews*, vol. 114, pp. 1–15, Oct. 2019.
- [25] L. Kaci *et al.*, "Solar inverter performance prediction," *2020 6th International Symposium on New and Renewable Energy (SIENR)*, Ghadaia, Algeria, pp. 1-5, 2021
- [26] F. Spertino *et al.*, "An experimental procedure to check the performance degradation on-site in grid-connected photovoltaic systems", *Proceedings of the 2014 IEEE 40th Photovoltaic Specialist Conference (PVSC)*, pp. 2600-2604, 2014

- [27] L. Aarniovuori, A. Kosonen, P. Sillanpää and M. Niemelä, "High-Power Solar Inverter Efficiency Measurements by Calorimetric and Electric Methods," in *IEEE Trans. on Power Electronics*, vol. 28, no. 6, pp. 2798-2805, June 2013.
- [28] E. Kuhn, C. Forgez, P. Lagonotte, and G. Friedrich, "Modelling Ni-mH battery using Cauer and Foster structures," *Journal of Power Sources*, vol. 158, no. 2, Spec. Iss., pp. 1490-1497, Aug. 2006.
- [29] Y. Li, "Electrochemical Impedance Spectroscopy Analysis of Lithium Ion Battery Based on Equivalent Circuit Model," 2020 2nd International Conference on Applied Machine Learning (ICAML), Changsha, China, 2020, pp. 282-285.
- [30] D. Gallo, C. Landi, M. Luiso and A. Rosano, "Experimental validation of mathematical models of storage systems for smart grids," *2013 IEEE International Workshop on Applied Measurements for Power Systems (AMPS)*, Aachen, Germany, 2013, pp. 126-131.
- [31] S. Scavuzzo, R. Guerrieri, A. Ferraris, A. Giancarlo Airale and M. Carello, "Alternative Efficiency Test Protocol for Lithium-Ion Battery," *2018 IEEE Intern. Conf.e on Environment and Electrical Engineering and IEEE Industrial and Commercial Power Systems Europe (EEEIC / I&CPS Europe)*, Palermo, Italy, 2018, pp. 1-5.
- [32] "PVZEN – PhotoVoltaic Zero Energy Network." Available online: <https://pvzen.polito.it/> (accessed Dec. 13<sup>th</sup>, 2024).
- [33] M. A. Bazilian, G. F. Rogner, M. Howells, and J. Hermann, "Assessing the potential impacts of COVID-19 on renewable energy systems: A perspective from the energy resilience field," *Energy*, vol. 202, pp. 117776, 2020.
- [34] Tao Jiang, Chenghao Wu, Tao Huang, Rufeng Zhang, Xue Li. Optimal Market Participation of VPPs in TSO-DSO Coordinated Energy and Flexibility Markets [J]. *Applied Energy*, 2024, 360, 122730.
- [35] F. Spertino et al., "Toward the Complete Self-Sufficiency of an nZEBs Microgrid by Photovoltaic Generators and Heat Pumps: Methods and Applications," *IEEE Trans. on Industry Applications*, vol. 55, no. 6, pp. 7028-7040, 2019.
- [36] "Photovoltaic Geographical Information System (PVGIS)." Available online: (accessed Dec. 13<sup>th</sup>, 2024).
- [37] S. B. Schujman et al., "Evaluation of protocols for temperature coefficient determination," Proc. 2015 IEEE 42nd Photovoltaic Specialist Conference (PVSC), New Orleans, LA, USA, 14-19 June 2015, pp. 1-4.
- [38] J. Muñoz, F. Martinez-Moreno, and E. Lorenzo, "On-site characterization and energy efficiency of grid-connected PV inverters," *Progress in Photovoltaics: Research and Applications*, vol. 19, pp. 192-201, 2011.
- [39] M. Murnane, A. Ghazel, "A Closer Look at State of Charge (SOC) and State of Health (SOH) Estimation Techniques for Batteries." Available online: <https://www.analog.com/media/en/technical-documentation/technical-articles/A-Closer-Look-at-State-Of-Charge-and-State-Health-Estimation-Techniques> (access. on 2023-12-1).
- [40] ISO 10012:2003 - *Measurement management systems - Requirements for measurement processes and measuring equipment*.
- [41] BIPM, IEC, IFCC, ILAC, ISO, IUPAC, IUPAP, and OIML, *Evaluation of Measurement Data - Guide to the Expression of uncertainty in Measurement*, document JCGM 100:2008, 2008.
- [42] ISO/TS 28037:2010 - *Determination and use of straight-line calibration functions*.
- [43] A. Mazza and G. Chicco, "High-Quality Load Pattern Reconstruction from Smart Meter Data to Enhance the Assessment of Peak Power and Network Losses," in *IEEE Transactions on Industry Applications*, vol. 58, no. 3, pp. 3261-3274, May-June 2022.
- [44] F. Mavromatakis, F. Vignola, B. Marion, Low irradiance losses of photovoltaic modules, *Solar Energy*, Vol. 157, pp. 496-506, 2017.